Enzymatic Glucose Biosensor Based on Multiwalled Carbon Nanotubes-Zinc Oxide Composite

Selvakumar Palanisamy, Srikanth Cheemalapati, Shen-Ming Chen[*]

Department of Chemical Engineering and Biotechnology, National Taipei University of Technology, No. 1, Section 3, Chung-Hsiao East Road, Taipei 106, Taiwan, ROC
[*]E-mail: smchen78@ms15.hinet.net

An amperometric glucose biosensor based on multiwalled carbon nanotubes (MWCNT)-zinc oxide (ZnO) composite modified glassy carbon electrode (GCE) was demonstrated. ZnO micro sponges were electrochemically grown on MWCNT modified GCE at room temperature. GOx immobilized at MWCNT/ZnO composite modified GCE showed a pair of stable and well-defined reversible redox peaks, with a formal potential ($E^{0'}$) of −0.426 V, characteristic features of active redox couple of GOx. Fast electron transfer kinetics has occurred at the composite film, which was revealed from the high electron transfer rate constant (k_s) value of 1.66 s^{-1} and smaller peak-to-peak separation (ΔEp) value of 48 mV. The resulting biosensor shows good electrocatalytic activity towards glucose in short time (>5 s) at 0.32 V in the presence of ferrocene monocarboxilic acid (FMCA), which mediates the glucose oxidation. The fabricated biosensor showed linear range of 0.2-27.2 mM with a detection limit of 20 μM and a sensitivity of 4.18 μA/ mM. Moreover, good recovery results (~98 %) were achieved for spiked glucose concentrations in urine samples. In addition, the biosensor exhibited acceptable reproducibility, repeatability, good selectivity and storage stability.

1. INTRODUCTION

In the last half decade, researches on glucose monitoring have been attractive in various fields, especially in medical diagnostics, pharmaceuticals, and food processing [1-2]. Owing to the importance of glucose, the sensitive, selective and stable determination of glucose is mandatory and highly appreciable. Glucose oxidase (GOx) is the model enzyme used in amperometric biosensors for highly selective and sensitive glucose monitoring [3-5]. There are numerous reports available for glucose biosensor based on various materials modified electrodes, especially on carbon nanotubes (CNT) [6], graphene [7], metal nanoparticles [8] and conducting polymers [9]. Amid various materials,

MWCNT is a special material for GOx entrapment, because of its high electrocatalytic property and fast electron transfer rate towards GOx [10-11]. In recent years, many metal oxides have attracted considerable attention for the development of glucose biosensors [12-17]. Among various metal oxides, zinc oxide (ZnO) has gained special attention due to its wide band cap, semiconducting and piezoelectric properties. It also has a high isoelectric point (IEP~9.5), which facilitates the adsorption of negatively charged GOx (IEP~4.2) enzyme at physiological pH [18-19]. In the past few years, ZnO nano and micro structures have been prepared by various methods, such as electrodeposition [20-21], hydro thermal [22-25] and thermal decomposition method [26-28]. Electrodeposition methods have certain advantages over other methods for immobilization GOx at MWCNT/ZnO matrix, such as being cost effective and facile preparation of ZnO [29].

In our previous work, we electrochemically deposited ZnO micro flowers on reduced graphene oxide (RGO) modified glassy carbon electrode (GCE) [30-31]. In this report, we present a simple electrodeposition method of ZnO microsponges on MWCNT modified GCE for GOx immobilization. We described a facile method to construct glucose biosensor while being effective for the detection of glucose with good selectivity and sensitivity, which is ascribed to the large surface area as well as the synergistic effect of MWCNT and ZnO. MWCNT/ZnO micro-sponges provides flexible microenvironment platform for immobilization of GOx at philological pH, due to its strong electrostatic interactions between positively charged MWCNT/ZnO composite and negatively charged GOx, which could retain its bioactivity.

2. EXPERIMENTAL

2.1 Chemicals

MWCNTs with the lengths of 0.1-10 μm were obtained from Aldrich. GOx, type X-S from Aspergillus niger from Sigma-Aldrich and used as received. Zinc nitrate hexa hydrate, $(Zn (NO_3)_2 . 6H_2O)$ and potassium nitrate, (KNO_3) were obtained from Sigma-Aldrich. D (+) glucose (Dextrose, anhydrous) was purchased from Wako pure chemical Industries, Ltd. Ferrocene mono carboxylic acid (FMCA) was obtained from Alfa Aesar. The supporting electrolyte used for all experiments was pH 7 phosphate buffer solution (PBS), which was prepared by using 0.05 M Na_2HPO_4 and NaH_2PO_4 solutions. All other chemicals were of analytical grade and used without further purification.

2.2 Apparatus

A CHI 750A electrochemical workstation (CH Instruments) was employed for the cyclic voltammetry and amperometric studies. Surface morphological studies were carried out using Hitachi S-3000 H scanning electron microscope (SEM). Amperometric (i-t curve) measurements were performed using CHI-750a potentiostat with analytical rotator AFMSRX (PINE instruments, USA). A Conventional three-electrode system consisting of a modified GCE was used as the working electrode (active surface area = 0.079 cm^{-2}), an Ag/AgCl electrode (Sat. KCl) as the reference electrode and a

platinum wire with 0.5 mm diameter as the counter electrode was employed for electrochemical experiments. All measurements were carried out at room temperature and solutions in the electrochemical cell were kept under nitrogen (N_2) atmosphere.

2.3 Fabrication of modified electrodes

Prior to modification, the GCE was first polished with alumina slurry, followed by successive sonication in ethanol and double distilled water. After bath sonication the electrode was rinsed with double distilled water and allowed to dry at room temperature. MWCNT (0.1g/ml) was dispersed well in dimethylformamide (DMF) followed by sonication for 2 h. About 8μl of MWCNT (optimized concentration) was carefully drop casted on the pre-cleaned GCE and dried in room temperature. Subsequently, the MWCNT modified GCE was shifted to an electrochemical cell containing 0.05 M $(ZnNO_3)_2.6H_2O$ and KNO_3 solution. 30 successive cyclic voltammograms were performed in the potential range of 0 to -1.5 V at the scan rate of 50 mV s^{-1}. After 30 consecutive cycles, ZnO was electrochemically deposited on MWCNT modified GCE resulting in MWCNT/ZnO composite formation.

The fresh GOx solutions were prepared by using PBS (pH 7) and stored in refrigerator when not in use. In order to immobilize GOx on the as-prepared MWCNT/ZnO composite modified GCE, about 8 μl GOx (optimized concentration) was drop casted and allowed to dry at room temperature. The negatively charged GOx interacted with the positively charged MWCNT/ZnO matrix. Thus, immobilization of GOx on MWCNT/ZnO was highly favored through the electrostatic interactions. The obtained MWCNT/ZnO composite film modified GCE was then gently rinsed few times with doubly distilled water to remove the loosely bound GOx. The fabricated MWCNT/ZnO/GOx electrode was used for further experiments and stored in 4ºC under dry condition when not in use.

3. RESULTS AND DISCUSSIONS

3.1 Electrochemical formation mechanism of MWCNT/ZnO composite

The MWCNT modified GCE was transferred to an electrochemical cell containing 0.05 M $(ZnNO_3)_2.6H_2O$ and KNO_3 solution in N_2 atmosphere. 30 successive cyclic voltammograms were performed in the potential range between 0 and -1.5 V at the scan rate of 50 mVs^{-1} (see Fig.1). During the first anodic potential scan, with an onset potential of -0.83 V, a small anodic hump appears at -0.66 V, indicating the dissociation of zinc nitrate and the analogous formation of Zn^{2+} ions [30]. Relatively, no anodic peak was observed at MWCNT/GCE in the same potential window. Therefore, the anodic peak noticed at MWCNT/ ZnO/GCE was attributed to the Zn^{2+} ions. During the second cathodic potential scan, at more negative potential (~1V), the as dissociated NO_3^- ions had undergone further reduction forming both NO_2^- ions and oxygen. Meanwhile, the released oxygen was captured by the anchored Zn^{2+} ions, resulting in the formation of MWCNT/ZnO composite (step 1).
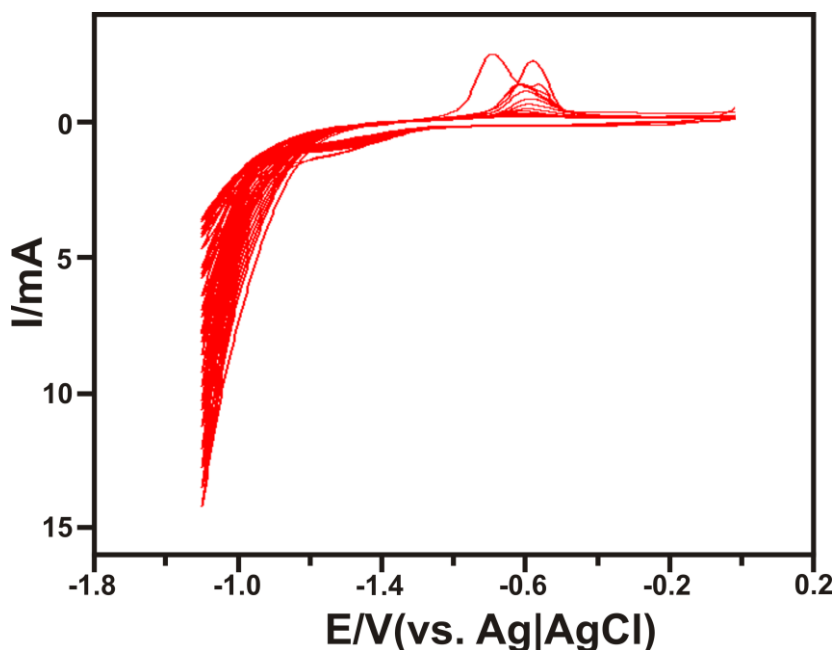
Figure 1. 15 consecutive cyclic voltammograms recorded at a MWCNT modified GCE in 0.5 mM $(ZnNO_3)_2 \cdot 6\,H_2O$ and 0.5 mM KNO_3 containing N_2 saturated 0.05 M PBS (pH 7) at the scan rate of 50 mV s^{-1}.

As reported previously, ZnO electrochemical deposition conceivably occurs by any one of the following reversible mechanistic pathways [32-33]

$$Zn^{2+} + NO_3^- + 2e^- \rightarrow ZnO + NO_2^- \tag{1}$$

$$Zn^{2+} + \tfrac{1}{2}\,O_2 + 2e^- \rightarrow ZnO \tag{2}$$

3.2 Direct electrochemistry of GOx

Cyclic voltammetry was employed to study the performance of the fabricated biosensor. The direct electrochemistry of GOx immobilized MWCNT/ZnO modified electrode was investigated in deoxygenated PBS (pH 7). Fig. 2 shows the cyclic voltammograms (CV) obtained at bare (a), MWCNT (b), MWCNT/ZnO (c) and MWCNT/ZnO/GOx (d) film modified GCEs in deoxygenated PBS at the scan rate of 50 mV s^{-1}. Cyclic voltammograms were recorded in the potential range of −0.85 to 0.05 V. Bare GCE, MWCNT and MWCNT/ZnO GCEs exhibited no electrochemical signals. It should be noted that MWCNT/ZnO/GCE has higher active electrode area than that of MWCNT/GCE, as evident from the high background current observed at the former. MWCNT/ZnO/GOx electrode shows a pair of well-defined reversible redox peaks at −0.450 V and −0.402 V with the peak-to-peak separation (ΔE_p) of 48 mV at 50mVs^{-1}. This is characteristic peak of reversible electron transfer process of redox active center (FAD/FADH$_2$) in the GOx [34-35]. MWCNT/ZnO plays a key role in facilitating the direct electron transfer of GOx and the electrode

surface. It revealed that the synergetic effect of MWCNT/ZnO played an important role in facilitating the direct electron transfer of GOx. The fast electron transfer of GOx can be attributed to the good biocompatibility, large surface area, and high electronic communication capability of MWCNT/ZnO composite.
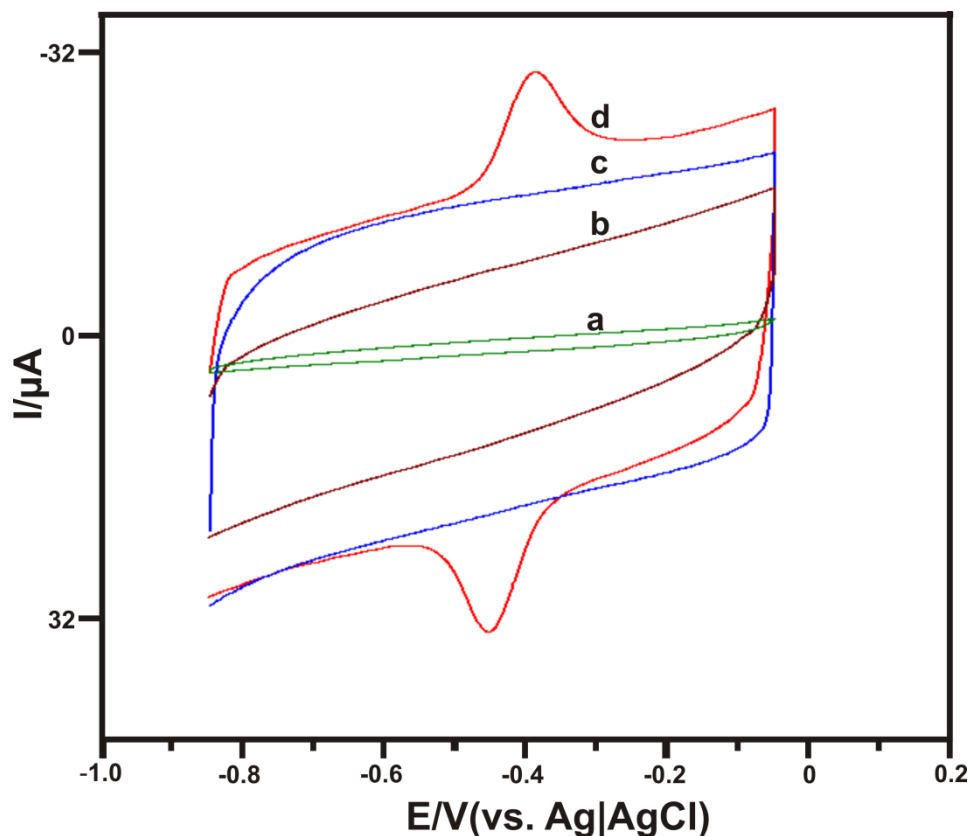
Figure 2. (A) Cyclic voltammograms obtained at bare GCE (a), MWCNT (b), MWCNT/ZnO (c), and MWCNT/ZnO/GOx (d) film modified GCEs in deoxygenated PBS at 50 mV s^{-1} scan rate.

3.2 Effect of scan rate and pH at MWCNT/ZnO/GOx modified electrode

The effect of scan rate on the voltammetric response of GOx on MWCNT/ZnO/GOx in deoxygenated PBS also has been studied as shown in Fig. 3A. Upon increasing the scan rates, the redox peak currents and peak separation increased linearly. Meanwhile the cathodic and anodic peak potentials showed a small shift with the subsequent increase in the peak to peak separation. The cathodic and anodic peak current (I_{pc} and I_{pa}) shows a linear relationship with the scan rate between 0.01 and 0.1 Vs^{-1} (Fig.3A inset). This demonstrates that the redox reaction of GOx at the MWCNT/ZnO composite GCE is a surface-controlled process, not a diffusion controlled process. The electron transfer rate constant (k_s) was estimated as 1.66 s^{-1} according to the Eq.3 by Laviron [36]. The obtained k_s value was larger than that of GOx adsorbed on carbon nanotubes electrode (1.08 s^{-1}) [37], and GOx immobilized on MWCNTs–gold colloid–poly (diallyldimethylammonium chloride) (PDDA)

(1.01 s^{-1}) [38] reported previously. These results confirm that, the synergetic effect of MWCNTs and ZnO plays an important role to facilitate electron transfer between GOx and the electrode surface.

$$Log\ K_s = \alpha\ Log(1-\alpha) + (1-\alpha)Log\ \alpha - Log\left(\frac{RT}{nFv}\right) - \frac{\alpha(1-\alpha)\ nF\Delta E_p}{2.3RT} \qquad (3)$$

The direct electrochemical reaction of FAD/FADH$_2$ at GOx is a two protons (2H$^+$) coupled with two electrons (2e$^-$) process.
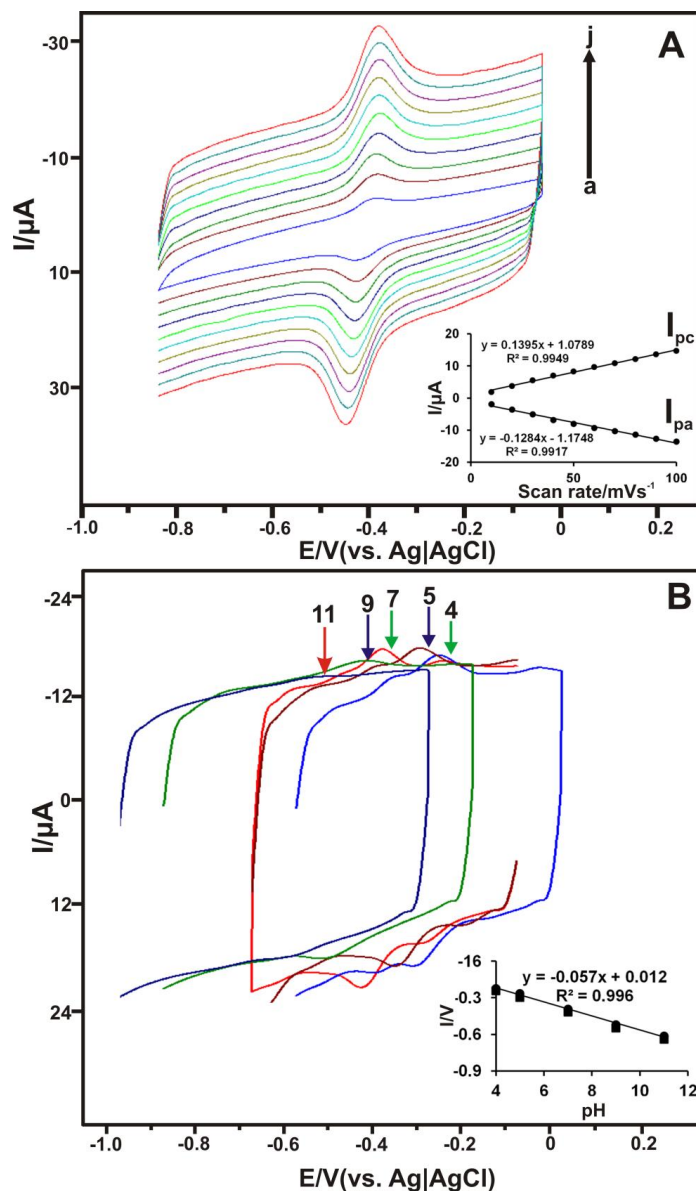
Figure 3. (A) Cyclic voltammograms recorded at MWCNT/ZnO/GOx composite film modified GCE in deoxygenated PBS at different scan rates. The scan rates from inner to outer are: 10 to 100 mV s^{-1} (a-j). Inset shows the linear dependence of I$_{pa}$ and I$_{pc}$ on scan rate (a to 100 mV s^{-1}). (B) Cyclic voltammograms obtained at MWCNT/ZnO/GOx composite film modified GCE in deoxygenated various buffer solutions (pH 4–9) at the scan rate of 100 mV s^{-1}. Inset shows the influence of pH on E$_{pa}$ and E$_{pc}$ of MWCNT/ZnO/GOx composite film.

Therefore, the pH value has considerable influence on the electrochemical behavior of MWCNT/ZnO/GOx, this was investigated as shown in Fig. 3B. The formal potential ($E^{0'}$) shifted negatively of both anodic and cathodic peaks upon increasing the pH and it exhibited a linear dependence on the pH range of 4.0-11.0 with a slope of −57 mV/pH (0.996). The slope value was found to be very close to the theoretical value of –59 mV/pH at 25°C for a reversible electron transfer coupled proton transport process with equal number of protons and electrons according to the reaction in Eq.3 [39-40, 43]. This result also implied that the redox reaction of GOx is a two protons (H^+) and two electrons (e^-) process.

$$GOx + FAD + 2\,e^- + 2\,H^+ \leftrightarrow GOx - FADH_2 \qquad (4)$$

3.3 Surface morphological study
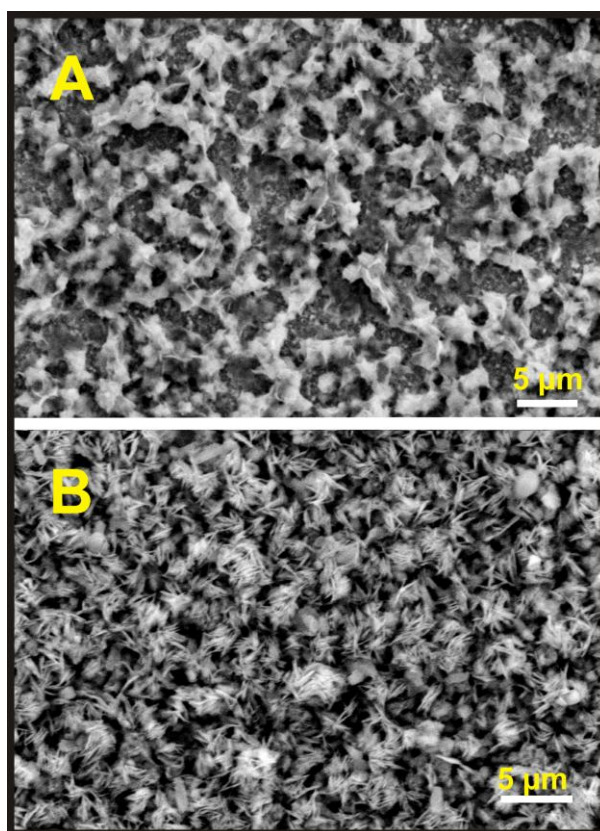
Figure 4. SEM images of electrochemically deposited ZnO micro-sponges on MWCNT at room temperature (A) and GOx immobilized at MWCNT/ZnO composite (B)

Fig. 4A shows the typical SEM images of the as grown ZnO micro-sponges by electrochemical deposition on MWCNT surface. It can be seen that the as-grown ZnO microstructures were in between 500 nm to 1μm in size. It is also noted that the individual ZnO micro-sponges were interconnected through MWCNT networks. We believe that, initially the ZnO growth should have headed in longitudinal direction along the MWCNT walls, as they served as potential templates. Later on, the as

deposited ZnO particles should have acted as seeds, further growth process progressing in longitudinal direction, leading to the formation of ZnO-micro-sponges. The large surface area of MWCNT/ZnO composite and the net positive surface charges are profitable for immobilizing negatively charged GOx. As shown in Fig. 4B, GOx has been uniformly loaded above the MWCNT/ZnO surface, indicating the typical coral reefs like structure formation. Fig. 4B also provides evidence that bead like GOx structures have been anchored above the coral reefs.

3.4 Electrocatalysis of MWCNT/ZnO/GOx composite film towards glucose oxidation and oxygen reduction
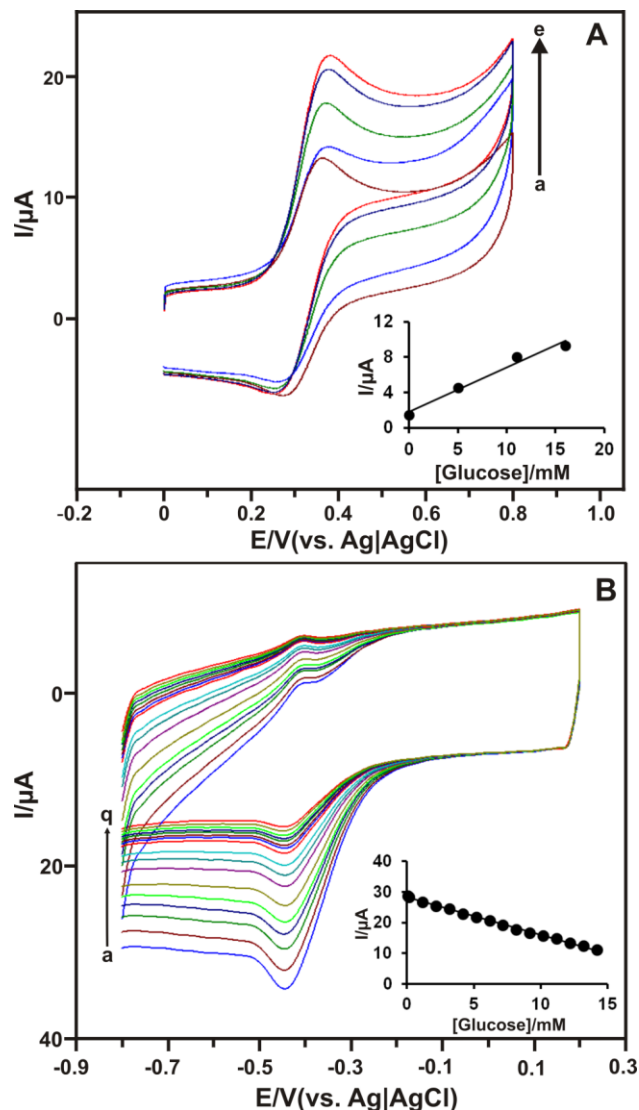
Figure 5. (A) Cyclic voltammograms recorded at MWCNT/ZnO/GOx composite film modified GCE (a) without and (b-e) with 0.02 - 16.24 mM glucose containing deoxygenated PBS with 1 mM FMCA. Scan rate: 50 mV s^{-1}. Inset plot shows the linear dependence of I$_{pa}$ vs. [glucose]/ mM. (B) Cyclic voltammograms recorded at MWCNT/ZnO/GOx composite film modified GCE (a) without and (b-q) with 0.05 – 14.24 mM glucose containing oxygenated PBS. Scan rate: 50 mV s^{-1}. Inset plot shows the linear dependence of peak current vs. [glucose]/ mM.

Fig. 5A shows the cyclic voltammograms of MWCNT/ZnO/GOx biosensor in the presence of different concentration of glucose in PBS (pH 7) containing 1 mM of FMCA. In the absence of glucose, pair of well-defined redox peaks was observed, featuring one electron redox reaction of Fc^+/Fc couple. Upon successive addition of different concentration of glucose (a-e), I_{pa} linearly increased, displaying a typical electro catalytic oxidation of glucose. Moreover, the calibration curve corresponding to cyclic voltammetry response (as inset in Fig. 5A) is linear against the concentrations of glucose ranging from 0.02 to 16.02 mM with a correlation coefficient of 0.975. This result shows that the MWCNT/ZnO/GOx film possesses higher electrocatalytic activity towards glucose, which was ascribed to the synergistic effect of MWCNT and ZnO as well as the well immobilized GOx.

In order to confirm the feasibility of the electrocatalytic activity of MWCNT/ZnO/GOx biosensor for glucose, the sensing strategy was investigated in oxygen saturated PBS (pH 7) in the negative potential range (0.2 to -0.8), as shown in Fig.5B. It shows the CVs of MWCNT/ZnO/GOx GCE at different concentration of glucose in 0.05 M PBS (pH 7). The reduction current of GOx dramatically decreased linearly in the presence of glucose at about -0.44 V, due to the reduction of dissolved oxygen from the solution (Fig. 5B inset). It confirms that, the reduction of GOx (FAD) with respect to the glucose leads to the decrease of the reduction peak current linearly. It was found that the reduction peak current is linearly proportional to the concentration range from 0.05-14.15 mM glucose with correlation coefficients of 0.997. The mechanism of the reaction can be described as follows,

$$GOx\,(FAD) + \text{Glucose} \leftrightarrow GOx\,(FADH_2) + Glucolactone \tag{5}$$
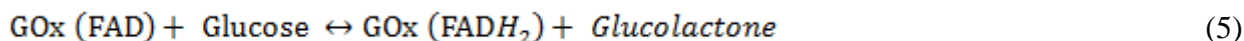
3.5 Amperometric determination of glucose at MWCNT/ZnO/GOx modified RDE

Amperometric i–t curve is the utmost used method to evaluate the electrocatalytic activity of enzyme-based biosensors. Fig. 6A depicts a typical amperometric curve for the MWCNT/ZnO/GOx modified rotating disc electrode (RDE, electrode active surface area=0.24 cm^{-2}) with successive addition of different concentration of glucose into 0.05 M PBS (pH 7) containing 1 mM FMCA under applied potential 0.32 V. Once the background current became stable, a different concentration solution of glucose was injected into the electrolytic cell constantly stirred at 1200 RPM, and its response was measured. The sharp shoulder peaks appeared immediately for the successive addition of different glucose concentrations (3 mM, 2 mM and 1 mM), as indicated by arrows in Fig. 6A. The shoulder peaks appeared as a result of glucose oxidation. With further increase in glucose addition, the glucose consumption increases and thus the catalytic current increases gradually and reached maximum current at a very high glucose concentration (25.84 mM). The reaction occurring in the biosensor responded rapidly of every addition of glucose level with different concentrations to reach the dynamic equilibrium, and the steady state current signal was found to be within 3-5 s. Thus indicating that, the composite film modified RDE has higher electro sensitivity towards the addition of glucose. The fabricated biosensor shows that the response current increased linearly between 0.2 and 27.2 mM of glucose (Fig. 6B). MWCNT/ZnO/GOx composite modified electrode has a sensitivity of 4.18 $\mu A\,mM^{-1}\,cm^{-2}$ with the slope value of (1.0028 ± 0.009) $\mu A\,mM^{-1}$ and a limit of detection (LOD)

of 0.02 mM (S/N=3). It is clear that MWCNT/ZnO/GOx composite modified electrode possesses good linear range (0.2– 27.2 mM), sensitivity and response time for glucose detection, which is significantly higher than other previously reported glucose biosensors based on different modified working electrodes (Table 1).
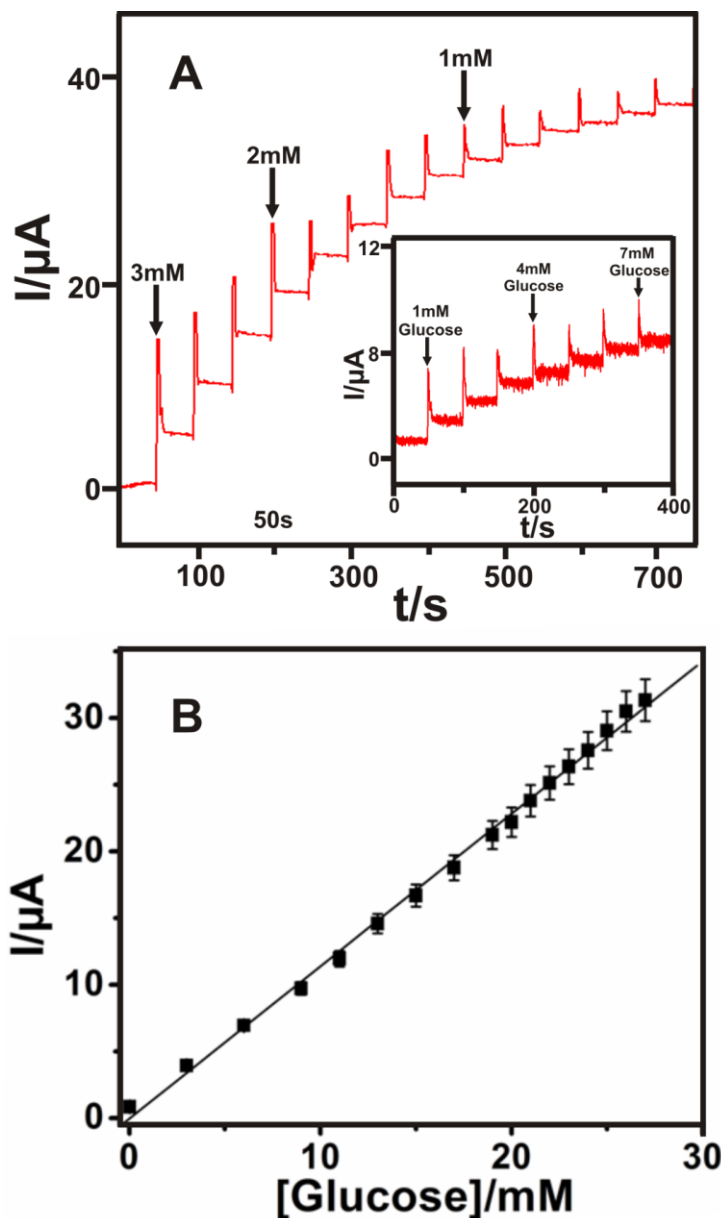
Figure 6. A) Amperometric i-t response at MWCNT/ZnO/GOx composite film modified rotating disc GCE upon successive additions of 0.02-27.2 mM glucose into continuously stirred N$_2$ saturated 0.05 mol L^{-1} PBS (pH 7) containing 1 mM FMCA. Applied potential: 0.32 V; Rotation rate: 1600 RPM. Inset shows that an amperometric response for successive addition of 1 mM glucose in same conditions B) Calibration curve of concentration of glucose versus current response, the calibration equation: Ip /μA = (1.0028 ± 0.001) /μA mM^{-1} + 0.0794 ± 0.0044. The slope value is (1.0028 ± 0.009) μA mM^{-1}.

The good catalytic activity towards glucose using the proposed biosensor is attributed due to its excellent conductivity, facile electron mobility of MWCNT and good biocompatibility of ZnO.

Table 1. Comparison of electroanalytical performance of various GOx based biosensors

Electrode	Sensitivity (μA cm^{-2} m mol L^{-1})	Linear range (mmol L^{-1})	K_s (s^{-1})	Response t/s	Ref.
Gelatin MWCNT[a]/GOx	2.47	6.3 - 20.09	1.08	-	[6]
CNT[b]/GOx	2.40	0.04 - 1	1.08	-	[37]
CNT/ Colloidal Au/PDDA[c]/GOx	2.50	0.5 – 5.2	1.01	-	[38]
MWCNT/Au/GOx	2.527	0.1 - 10	-	-	[41]
CNT/Polypyrrole/GOx	0.095	0.25 - 4	-	8	[42]
MWCNT/ZnO/GOx	4.18	0.2 – 27.2	1.66	>5	This work

[a] MWCNT-Multiwalled carbon nanotubes
[b] CNT-Carbon nanotubes
[c] PDDA- poly (diallyldimethylammonium chloride).

3.6 Anti-interference study
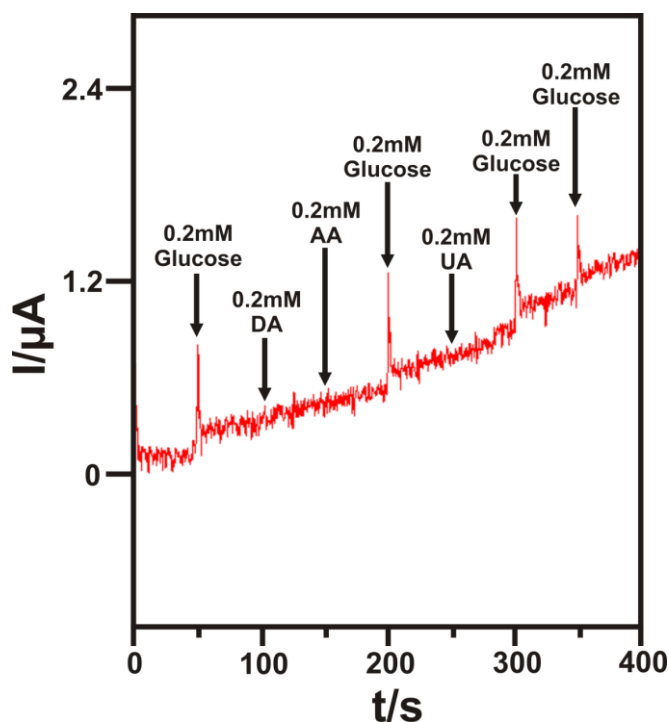
Figure 7. Amperometric i-t response at MWCNT/ZnO/GOx composite film modified rotating disc GCE for the successive addition of 0.2 mM Glucose, 0.2 mM AA, 0.2 mM DA, and 0.2 mM uric acid solutions into continuously stirred N$_2$ saturated 0.05 M PBS (pH 7) containing 1 mM FMCA. Applied potential: 0.32 V; Rotation rate: 1600 RPM.

In order to investigate the possible interfering electroactive species on the fabricated MWCNT/ZnO/GOx [44-48] modified RDE electrode, we monitored the response of the proposed biosensor with the addition of 0.2 mM ascorbic acid (AA), 0.2 mM uric acid (UA) and 0.2 mM dopamine (DA) [49-50] at different time intervals as shown in Fig. 7. The working potential was held at 0.32 V containing 1 mM FMCA in PBS (pH 7) at 1200 RPM. The addition of each electroactive interfering species brought out hardly discernible current response, whereas notable response was observed for 1 mM glucose (Fig. 7). These results validates that the electroactive species does not affect the response current of glucose and they are quite negligible. It suggests that MWCNT/ZnO/GOx composite film was highly selective for the detection of glucose.

3.7 Stability, repeatability and reproducibility

In order to investigate the storage stability of the MWCNT/ZnO/GOx biosensor, after each experiment the modified electrode was washed with pH 7 buffer and stored in a 2 mM glucose containing 1 mM FMCA in PBS (pH 7) at 4 °C, and its background current was tested periodically for 15 days. The sensitivity retained about 91.3% of glucose initial sensitivity up to 15 days, indicating the excellent storage stability of the MWCNT/ZnO/GOx composite film, and it can be used for minimum two weeks. The good biocompatibility of the MWCNT/ZnO composite and the strongly bounded GOx can be the likely reasons for the high stability. The repeatability and reproducibility of the proposed biosensors were evaluated by CV studies. The five electrodes fabricated independently showed an acceptable reproducibility with a relative standard deviation (RSD) of 4.43 % for each 2 mM glucose concentration. The RSD for each 2 mM glucose measurements (n=10) was 3.18 % revealing the good repeatability of the proposed biosensor.

3.8 Real sample analysis

Table 2. Determination of glucose from urine samples using spiking method

Sample	Glucose added (mmol L^{-1})	Glucose found (mmol L^{-1})	Recovery (%)	RSD (%)
1	2.0	1.968	98.4	2.25
2	4.0	1.953	97.7	3.28
3	6.0	1.942	97.1	4.04
4	8.0	1.952	97.6	3.38

The proposed sensor was tested in glucose containing urine samples by stand addition method. Urine samples used in this study were obtained from a healthy man. Prior to analysis, we diluted the urine sample at least 5 times using PBS (pH 7), without any further purification. Known concentration of glucose was spiked into human urine at regular intervals and the response at the composite film was observed using amperometric i-t technique (conditions are as same like section 3.5). The spiked (added) and found glucose concentrations along with recovery results was tabulated in the Table.2.

The good recovery results indicated that the proposed sensor can be effectively used for the real sample analysis to detect glucose.

4. CONCLUSIONS

In summary, we present the simple and cost effective one step electrodeposition of ZnO microsponges on MWCNT modified GCE. The direct electrochemistry of the model enzyme, GOx was revealed at the MWCNT/ZnO surface. The strong electrostatic interactions between positively charged MWCNT/ZnO composite and negatively charged GOx provides good stability to the immobilized GOx. The as-prepared MWCNT/ZnO/GOx composite film showed good catalytic activity for glucose oxidation in the presence of FMCA. Besides that, MWCNT/ZnO sensor is highly sensitive towards glucose and it holds acceptable selectivity. The proposed sensor holds a great potential for practical applications, as evident from the good recovery results achieved in the human urine samples. As a future perspective, we believe that MWCNT/ZnO composite material could be a promising electrode material for the immobilization of various redox enzymes or proteins based biosensors. The good performance characteristics of this glucose sensor also open up in favor of exploiting this composite electrode as a bioanode in fuel cell applications.

References

1. R.W. Keay, C.J. McNeil, *Biosens. Bioelectron*. 13 (1998) 963-970.
2. M. Musameh, J. Wang, A. Merkoci, Y. Lin, *Electrochem. Commun*. 4 (2002) 743–746.
3. S. Liu, H. Ju, *Biosens. Bioelectron*. 19 (2003) 177–183.
4. S.G. Wang, Q. Zhang, R. Wang, S.F. Yoon, *Biochem. Biophys. Res. Commun*. 311 (2003) 572–576.
5. X. Chen, S.J. Dong, *Biosens. Bioelectron.* 18 (2003) 999–1004.
6. A.P. Periasamy, Y.J. Chang, S.M. Chen, *Bioelectrochemistry* 80 (2011) 114–120.
7. Z. Wang, X. Zhou, J. Zhang, F. Boey, H. Zhang, *J. Phys. Chem*. C, 113 (2009) 14071–14075.
8. Y. Zoua, C. Xiang , L.X. Suna, F. Xu, *Biosens. Bioelectron*. 23 (2008) 1010–1016.
9. V. Bajpai, P. He, L. Goettler, J.H. Dong, L. Dai, *Synthetic Metals* 156 (2006) 466–469.
10. Y.T. Wang, L. Yu, Z.Q. Zhu, J. Zhang, J.Z. Zhu, C. Fan, *Sens. Actuators*, B 136 (2009) 332–337.
11. P. Norouzi, F. Faridbod, B. Larijani, M.R. Ganjali, *Int. J. Electrochem. Sci*., 5 (2010) 1213-1224.
12. H.N. Choi, M.A. Kim, W.Y. Lee, *Anal. Chim. Acta* 537 (2005) 179–187.
13. P. Norouzi1, H. Ganjali, B. Larijani, M.R. Ganjali1, F. Faridbod, H.A. Zamani, *Int. J. Electrochem. Sci.*, 6 (2011) 5189 - 5199.
14. J. Chen, W.D. Zhang, J.S. Ye, *Electrochem. Commun*. 10 (2008) 1268–1271.
15. J. Zang, C.M. Li, X. Cui, J. Wang, X. Sun, H.D. Chang, Q. Sun, *Electroanalysis* 19 (2007) 1008–1014.
16. Y. Li, X. Liu, H. Yuan, D. Xiao, D. *Biosens. Bioelectron*. 24 (2009) 3706–3710.

17. L.C. Jiang, W.D. Zhang, *Biosens. Bioelectron.* 25 (2010) 1402–1407.
18. J.X. Wang, X.W. Sun, A. Wei, Y. Lei, X.P. Cai, C.M. Li, Z.L. Dong, *Appl. Phys. Lett.* 88 (2006) 233106-233108.
19. S. Palanisamy, A.T. Ezhil Vilian, S.M. Chen, *Int. J. Electrochem. Sci.*, 7 (2012) 2153- 2163.
20. Q.P. Chen, M.Z. Xue, Q.R. Sheng, Y.G. Liu, Z.F. Ma, *Electrochem. Solid-State Lett.* 9 (2006) 58-61.
21. Y.L. Chen, Z.A. Hu, Y.Q. Chang, H.W. Wang, Z.Y. Zhang, Y.Y. Yang, H.Y. Wu, *J. Phys. Chem.* C 115 (2011) 2563–2571.
22. H. Sun, M. Luo, W. Weng, K. Cheng, P. Du, G. Shen, G. Han, *Nanotechnology* 19 (2008) 125603.
23. S. Yamabi, J. Yahiro, S. Iwai, H. Imai, *Thin Solid Films* 489 (2005) 23-30.
24. N. Wang, L. Jiang, H. Peng, G. Li, Cryst. *Res. Technol.* 44 (2008) 341-345.
25. C. Bingqiang, C.Weiping, Y. Li, F. Sun, L. Zhang, *Nanotechnology* 16 (2005)1734-1738.
26. D. Lupu, A.R. Biris, F. Watanabe, Z. Li, E. Dervishi, V. Saini, Y. Xu, A.S. Biris, M. Baibarac, I. Baltog, *Chem. Phys. Lett*. 473 (2009) 299–304.
27. A. Umar, Y.B. Hahn, *Nanotechnology* 17 (2006) 2174-2180.
28. G. Deng, A. Ding, W. Cheng, X. Zheng, P. Qiu, *Solid State Commun*. 134 (2005) 283-286.
29. F. Hu, S. Chen, C. Wang, R. Yuan, Y. Chai, Y. Xiang, C. Wang, *J. Mol. Catal. B: Enzym*. 72 (2011) 298– 304.
30. S. Palanisamy, S.M. Chen. R. Saraswathi, *Sens. Actuators*, B 166–167 (2012) 372–377.
31. S. Palanisamy, A.T. Ezhil Vilian, S. M. Chen˙ , *Int. J. Electrochem. Sci.*. 7(2012) 2153-2163
32. M. Izaki, T. Omi, *Appl.Phys. Lett*. 68 (1996) 2439-2440.
33. M. Izaki, T. Omi, *J. Electrochem. Soc*. 143 (1996) L53-L55.
34. C. Cai. J. Chen, *Anal. Biochem*. 332 (2004) 75–83.
35. X. Luo, A.J. Killard, M.R. Smyth, *Electroanalysis* 18 (2006) 1131–1134.
36. E. Laviron, *J. Electroanal. Chem*. 101 (1979) 19–28.
37. X. Luo, A.J. Killard, M.R. Smyth, *Electroanalysis* 18 (2006) 1131 – 1134.
38. Y.L. Yao, K.K. Shiu, *Electroanalysis* 20 (2008) 1542–1548.
39. N. Jia, L. Liu, Q. Zhou, L. Wang, M. Yan, Z. Jiang, *Electrochim. Acta* 51 (2005) 611– 618.
40. D. Wen, Y. Liu, G. Yang, S. Dong, *Electrochim. Acta* 52 (2007) 5312–5317.
41. B.Y. Wu, S.H. Hou, F. Yi, Z.X. Zhao, Y.Y. Wang, X.S. Wang, Q. Chena, *Biosens. Bioelectron*. 22 (2007) 2854–2860.
42. Y.C. Tsai, S.C. Li, S.W. Liao, *Biosens. Bioelectron.* 22 (2007) 495-500.
43. Y. Li, S. M. Chen, R. Sarawath, *Int. J. Electrochem. Sci.*. 6(2011) 3776-3788.
44. K.C. Lin, S.M. Chen, *Biosensors and Bioelectronics*, 21 (2006) 1737-1745
45. S. A. Kumar, H.W. Cheng, S.M. Chen, *Reactive and Functional Polymers*, 69 (2009) 364-370.
46. K.C. Lin, S.M. Chen, *J. Electroanal. Chem*., 578(2005) 213-222.
47. A. P. Periasamy, Y. H. Ho, S. M. Chen, *Biosensors and Bioelectronics*, 29(2011) 151-158.
48. S. M. Chen, K. T. Peng, *J. Electroanal. Chem*., 547,(2003), 179-189.
49. K. C. Lin, T. H. Tsai, S. M. Chen, *Biosensors and Bioelectronics*, 26(2010) 608-614
50. K. C. Lin, C. Y. Yin, S. M. Chen, *Int. J. Electrochem. Sci.*.6 (2011) 3951-3965